scientific reports

Check for updates

OPEN

SHC1 serves as a prognostic and immunological biomarker in clear cell renal cell carcinoma: a comprehensive bioinformatics and experimental analysis

Zhuangyu Guo[1,4], Congbo Cai[1,4], Kena Zhou[2], Lingmin Song[1], Xue Wang[1], Dongying Chen[3], Guobin Weng[1]✉ & Shuaishuai Huang[1]✉

SHC1 plays a crucial regulatory role in various tumors, but its significance in predicting prognosis and immune response in clear cell renal cell carcinoma (ccRCC) is yet to be determined. In this study, we conducted a bioinformatics analysis of SHC1 expression, prognosis, and immunological functions in ccRCC using multiple databases. The association between SHC1 and immune infiltration, immune escape, and immunotherapy in ccRCC was systematically established. In addition, we validated our results by western blot of tumor and adjacent-tumor samples from nine ccRCC patients, as well as three renal carcinoma cell lines compared to a normal renal cell line. Our analysis revealed that the mRNA expression level of SHC1 in ccRCC tissues is significantly higher than that in normal tissues. Consistently, western blot experiment showed ccRCC tissues and cell lines exhibit higher protein levels that normal tissues and cell lines. Importantly, patients with low expression of SHC1 demonstrated a higher survival rate, indicating that SHC1 could serve as an independent prognostic factor for predicting survival in ccRCC. Additionally, high expression of SHC1 was associated with increased severe immune cell infiltration, enhanced immune escape, and higher immunotherapy scores. Hence, SHC1 emerges as a novel and easily detectable biomarker for predicting clinical outcomes, immune escape, and immunotherapy response in patients with ccRCC.

Keywords SHC1, Clear cell renal carcinoma, Biomarker, Immune escape, Immunotherapy

Clear cell renal carcinoma (ccRCC) is a common and fatal type of renal cancer (RCC)[1–3]. Previous studies have shown that ccRCC is highly invasive in terms of immune and vascular infiltration[4,5]. Immuno-checkpoint blockade (ICB) and targeted therapies have significantly improved the survival rate of patients with advanced ccRCC[6]. However, identifying valuable predictors to distinguish patients who respond well to treatment remains crucial.

Recent studies have shown that immune genes were associated with immune infiltration and prognosis in ccRCC patients[7,8]. SHC1 (also known as SHCA) is an immune gene consisting of three subtypes (p46SHC, p52SHC, and p66SHC)[9]. Previous studies have shown that SHC1 influences tumorigenesis and proliferation through transcriptional activation of downstream signaling cascades such as RAS/MAPK and PI3K[10,11]. Additionally, recent studies have suggested that SHC1 might be involved in microenvironment and methylation alterations in various tumors, making it a promising immunotherapeutic target for cancer therapy[12–14]. SHC1 also regulated the expression of urinary exosome PTRF[15], which is non-invasive and more feasible in the clinic. However, there is a lack of research on SHC1 in the clinical treatment of ccRCC. Therefore, we need to further investigate the immune-infiltration and immunotherapeutic effects of SHC1 in ccRCC.

In this study, we comprehensively describe the expression levels of SHC1 in ccRCC and validate our findings by experiments using human samples and cell lines. Moreover, this study investigated the clinical significance

[1]Laboratory of Renal Carcinoma, Ningbo Urology and Nephrology Hospital, Urology and Nephrology Institute of Ningbo University, No.998 North Qianhe Road, Yinzhou District, Ningbo 315100, Zhejiang, China. [2]School of Medicine, Shanghai Jiao Tong University, Shanghai 200240, China. [3]Department of Community Work, Ningbo Yinzhou No.3 Hospital, Ningbo 315100, China. [4]These authors contributed equally: Zhuangyu Guo and Congbo Cai. ✉email: ddwgbin@aliyun.com; ss.huang@aliyun.com

and immune infiltration of SHC1 in ccRCC. The response to immune escape and ICB therapy of SCH1 in ccRCC was analyzed via Tumor Immune Dysfunction and Exclusion (TIDE) and The Cancer Immunome Atlas (TCIA). Our aim is to provide evidence for the development of new targeted therapies in ccRCC.

Materials and methods

Databases, patients and cell lines

The experimental database utilized in this study was the KIRC cohort. Clinical information and the RNA-seq data (KIRC, N = 72, T = 532) of this cohort were obtained from the TCGA website (https://portal.gdc.cancer.gov/). External validation databases included the International Cancer Genome Consortium (ICGC) database (RECA-EU, N = 45, T = 91. http://dcc.icgc.org) and the GEO database (GSE40435, N = 101, T = 101. https://www.ncbi.nlm.nih.gov/geo/). Table 1 displayed the clinical data from each database. The expression levels of SHC1 in tissues and cell lines were obtained from the GTEx website (https://gtexportal.org/home/) and the CCLE website (https://sites.broadinstitute.org/ccle).

Tissue samples were collected from nine ccRCC patients recruited from Ningbo Urology and Nephrology Hospital (NBUNH). This study was approved by the Ethics Committee of NBUNH and written informed consent was obtained from all included patients. The 786-O, ACHN, OS-RC-2 and HK-2 cell lines were purchased from the National Collection of Authenticated Cell Cultures (Shanghai, China). ACHN and HK-2 cells were cultured using DMEM (HyClone, Logan, Utah, USA), while 786-O and OS-RC-2 cells were cultured with RPMI-1640 medium (HyClone). All cells were cultured in a CO_2 incubator at a constant temperature of 37 °C.

mRNA expression levels and immunohistochemistry in tissues and cell lines

The R packages of "ggplot2" and "ggpubr" were applied to draw boxplots, comparing the mRNA expression levels of SHC1 in the experimental cohort and external databases. The R packages of "plyr" and "ggpubr" were used to map the expression levels of SHC1 in different human normal tissues and in various tumor cell lines. The R package of "GOplot" was used to graph the expression of SHC1 in ccRCC cell lines. The Human Protein Atlas website (https://www.proteinatlas.org/) was utilized to validate the protein expression level of SHC1.

For clinical samples or cells, total RNA was extracted by E.Z.N.A.® Total RNA Kit (Omega Bio-Tek, Norcross, GA, USA). A total of 1 μg RNA was reverse-transcribed into cDNA using ABScript II RT Master Mix (ABclonal, Woburn, USA). Real-time quantitative polymerase chain reaction (RT-qPCR) was performed on a 7500 real-time PCR system with 2X Universal SYBR Green Fast qPCR Mix (ABclonal, Woburn, USA) according to the manufacturer's instructions. The primer sequences utilized were as follows: The forward primer for SHC1 was 5′-GAACAAGCTGAGTGGAGGCG-3′ and the reverse primer was 5′-CCATGTACCGAACCAAGTAGGAA-3′. The forward and reverse primers for GAPDH were 5′-GGAAGCTTGTCATCAATGGAAATC-3′ and 5′-TGA TGACCCTTTTGGCTCCC-3′, respectively. Relative gene expression was normalized to that of GAPDH and the $2^{-\Delta\Delta Ct}$ method was used to calculate the relative expression levels of SHC1.

Western blot and cell cultures

Lysis was performed using RIPA buffer (Cat#R0010, Solarbio) containing 1% protease inhibitor PMSF for 5 min on ice. The lysate was subsequently centrifuged at 12,000 rpm for 10 min. The protein concentration was determined using the BCA method. Equal protein concentrations (25 μg) were separated on a 12% SDS-PAGE. The proteins were then transferred onto PVDF membranes (Millipore, Billerica, MA) and blocked for 1.5 h with 5% (w/v) non-fat dry milk at room temperature. Membranes were incubated with rabbit SHC1 (Cat#ab33770,

Characteristics	TCGA N = 532	ICGC N = 91	GSE40435 N = 101
Age category			
< 65/ ≥ 65/NA	333/199	57/34	51/50
Gender			
Male/Female	345/187	52/39	59/42
Vital status			
Alive/Dead	357/175	61/30	NA
Grade			
G1/G2/G3/G4/NA	14/228/206/76/8	NA	22/47/24/8
Tumor stage			
I/II/III/IV/NA	266/57/123/83/3	NA	NA
T stage			
T1/T2/T3/T4/NA	272/69/180/11	NA	NA
M stage			
M0/M1/MX	421/79/32	NA	NA
N stage			
N0/N1/N2/NA	240/16/0/276	NA	NA

Table 1. Summary of the clinical characteristics of ccRCC patients. *NA* clinical data are unknown.

Abcam) and rabbit GAPDH (Cat#5714s, CST) antibodies, respectively, at 4 °C overnight. Next, the membranes were washed three times with TBST, after which they were probed with Goat Anti-rabbit HRP-coupled secondary antibody (Cat#BA1055, Boster) for 1.5 h at room temperature. Finally, protein bands were visualized using an enhanced chemiluminescence reagent (Cat#180810-45, Advansta) and analyzed by Tannon GIS software.

Clinical relevance

According to the clinical information and expression data from TCGA, the R package of "ComplexHeatmap" was used to create heatmaps and subsequently compare differences in traditional clinicopathological parameters between the high and low SHC1 expression groups. Univariate and multivariate Cox regression analyses were conducted using the "survival" package to assess the independence of SHC1 from traditional clinical factors. The survival rates of the SHC1 high- and low-expression groups were graphed using the "survival" and "survivminer" packages. A nomogram was constructed using the 'regplot' and 'rms' packages to display the association between SHC1 expression and other clinical parameters for predicting 1-, 3-, 5-, and 8-year overall survival (OS).

Function and pathway analysis

Based on the criteria of a |Pearson correlation coefficient|> 0.50 and $P < 0.001$, we identified 164 genes related to SHC1. Supplementary 1 provides further details. The R packages of "clusterProfiler", "org.Hs.eg.db", "enrichplot", "ggplot2", "R.Utls" and "pathview" were used to analyze and plot pathways via gene ontology (GO) and Kyoto Encyclopedia of Genes and Genomes (KEGG). For gene set enrichment analysis, we searched MSigDB gene sets (http://software.broadinstitute.org/gsea/msigdb/index.jsp) of "c5.go.v7.4.symbols.gmt" and "c2.cp.kegg.v7.4.symbols.gmt" to study the situation in KIRC for various functions in different SHC1 expression groups.

Tumor immune infiltration

To analyze tumor immune infiltration, we utilized two different methods to confirm our findings. The CIBERSORT algorithm was employed to examine the relationship between SHC1 expression and 22 kinds of immune cells, visualized through a bar diagram. The ssGSEA algorithm could comprehensively quantified the relative abundance of immune cell types, pathways, functions, and checkpoints in each patient based on 29 immune gene sets (infiltration scores of 16 immune cells and activity of 13 immune-related pathways). The GSVA package was used to compare the differences between the high and low SHC1 expression groups.

Prediction of immune escape and immune response

Box plots were used to illustrate the relationship between SHC1 expression and immune checkpoints. The TIDE database (http://tide.dfci.harvard.edu) was employed to evaluate immune escape. To explore potential immune functions in high- and low-SHC1 expression groups, expression matrices were uploaded to the TIDE website. Additionally, immune phenotype scores from the TCIA (https://tcia.at/) were used to evaluate the immune properties of two immune checkpoint inhibitors (ICIs): CTLA4 and PD1, under varying expression levels of SHC1.

Statistical analysis

All statistical analyses were performed by R software version v4.1.1 (https://www.r-project.org/). A P value < 0.05 was considered to be statistically significant. We have marked * to clarify the different values, where * means $P < 0.05$, ** means $P < 0.01$, and *** means $P < 0.001$.

Ethics approval and consent to participate

The study was conducted in accordance with the Declaration of Helsinki. It was approved by the Ethics Committee of the Ningbo Urology and Nephrology Hospital (No.2023020). Written informed consent has been obtained from the patient(s) to publish this paper.

Results

SHC1 expression in multiple databases and renal human cohort

The mRNA expression of SHC1 was significantly higher in tumor tissues compared to in adjacent normal tissues ($P < 0.001$, Fig. 1A) based on data from TCGA KIRC database. Paired box plots also showed similar results ($P < 0.001$, Fig. 1E). These results were further validated by external databases of ICGC RECA-EU, GEO GSE40435 and our database of Ningbo Urology and Nephrology Hospital (NBUHN) ($P < 0.001$, Fig. 1B–D, F–H). Besides, western blot analysis of renal human tissues collected from NBUNH revealed that SHC1 expression was higher in ccRCC samples than that in their adjacent cancer tissues (Fig. 1I). These results suggest that SHC1 plays a pivotal role in the development of ccRCC.

mRNA expression of SHC1 in different tissues and cell lines

According to the data from the GTEx, SHC1 expression is relatively low in kidney tissues compared to other normal organs of the human body (Fig. 2A). However, CCLE database shows that SHC1 expression is relatively high in renal tumor cell lines compared to other organs (Fig. 2B). Among renal tumor cell lines, KMRC3 and TUHR10TKB cells exhibit the highest expression level of SHC1, while UMRC3 and UMRC7 show the lowest levels (Fig. 2C). Compared with HK-2 cells, the mRNA and protein expression levels of SHC1 are significantly higher in OS-RC-2, ACHN and 786-O (Fig. 2D,E).

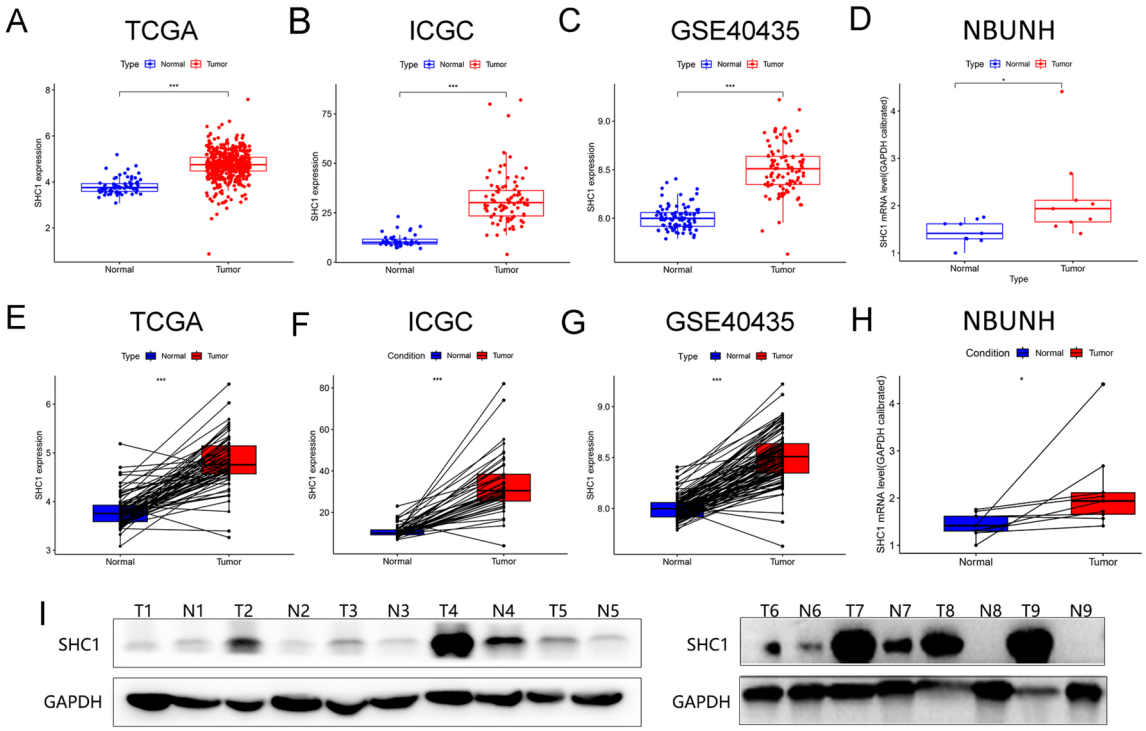

Fig. 1. Expression levels of SHC1 in ccRCC. (**A**) mRNA expression of SHC1 in TCGA KIRC (T = 532, N = 72). (**B**) mRNA expression of SHC1 in ICGC RECA-EU (T = 91, N = 45). (**C**) mRNA expression of SHC1 in GEO GSE40435 (T = 101, N = 101). (**D**) Boxplot of SHC1 expression in the NBUNH dataset (N = 9, T = 9); (**E**) Paired boxplot of the SHC1 mRNA expression in TCGA ccRCC (T = 72, N = 72). (**F**) Paired boxplot of the SHC1 mRNA expression in ICGC RECA-EU (T = 45, N = 45). (**G**) Paired boxplot of SHC1 mRNA expression in GEO GSE40435 (T = 101, N = 101). (**H**) Boxplot of paired SHC1 expression levels in the NBUNH dataset (N = 9, T = 9). (**I**) SHC1 protein expression in 9 paired samples from ccRCC patients. $^{*}P < 0.05$;$^{**}P < 0.01$;$^{***}P < 0.001$; ns, not significant.

The protein expression of SHC1 verified by immunohistochemistry

Immunohistochemistry analysis was used to validated the protein expression level of SHC1 in ccRCC tissues. SHC1 was found to be moderately low or not expressed in normal glomerular tissue (medium expression 3/9, low expression 3/9, no expression 3/9), while it was moderately highly expressed in renal tubules (high expression 3/9, medium expression 6/9) (Fig. 3A). In tumor tissues, the expression of SHC1 in tumor tissues was 2.9% high, 42.9% medium, 48.6% low, and 5.7% none (Fig. 3B). The immunohistochemistry finding supports our western blot result, indicating elevated SHC1 expression in ccRCC.

Clinical significance of SHC1

Patients with ccRCC in the TCGA cohort can be divided into high- and low-expression groups according to the median expression of SHC1. The results indicated that increased expression of SHC1 was correlated with worse stage, T stage and M stage ($P < 0.05$). Moreover, there were no significant differences between the high and low SHC1 expression groups in terms of age, gender and grade ($P > 0.05$, Fig. 4A). SHC1 was identified as an independent prognostic indicator for overall survival time (OS) in ccRCC after univariate and multivariate Cox analyses ($P < 0.05$, Fig. 4B,C). The Kaplan–Meier curve showed that patients with low SHC1 expression have better OS and progression-free survival (PFS) than those with high SHC1 expression ($P < 0.01$, Fig. 4D,E). Additionally, we developed a nomogram based on ccRCC data from the TCGA cohort to predict OS accurately and effectively. The results indicated that ccRCC patients with high SHC1 expression are more likely to advance to later stages, develop metastases and have a worse OS than those with low expression of SHC1 (Fig. 4F).

Correlation and functional analysis of SHC1

After correlation analysis, a total of 164 genes related to SHC1 were identified. These genes will be further analysed using GO and KEGG analysis. GO consists of biological process (BP), cell component (CC) and molecular function (MF), whose details are shown in S2 (Supplementary 2). BP comprises of extracellular matrix organization and extracellular structure organization, etc. CC involved focal adhesion and cell-substrate junction, ect. MF contains collagen binding and actin binding and so on (Fig. 5A). KEGG mainly discusses focal adhesion and diabetic cardiomyopathy (Fig. 5B), and more details can be seen in S3 (Supplementary 3). Five signaling pathways showed significant enrichment in different SHC1 expression phenotypes with the help of GSEA analysis in the gene sets of "c5.go.v7.4.symbols.gmt" and "c2.cp.kegg.v7.4.symbols.gmt" (Supplementary 4 and

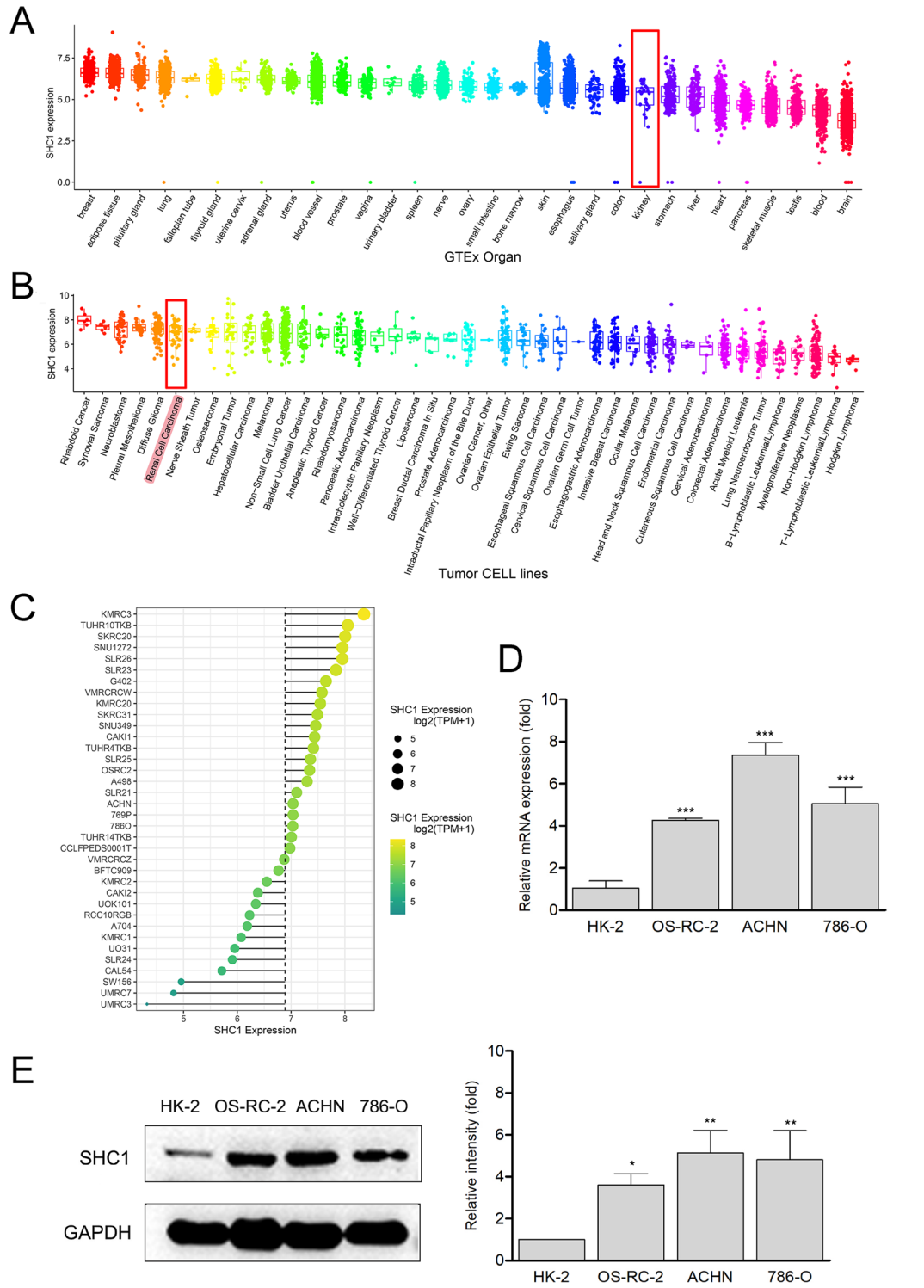

Fig. 2. Expression of SHC1 in normal organs and tumor cell lines. (**A**) mRNA expression of SHC1 in various normal organs of the human body. The red box refers to a normal kidney. (**B**) mRNA expression of SHC1 in various human cancer cell lines, with the red box highlighting renal cancer cell lines. (**C**) mRNA expression of SHC1 in 36 ccRCC cell lines. Green represents low expression and yellow represents high expression. The size of the circle represents the amount of expression. mRNA (**D**) and protein (**E**) levels of SHC1 in three renal carcinoma cell lines (OS-RC-2, ACHN and 786-O) and a normal renal cell line (HK-2). $^{*}P<0.05$, $^{*}P<0.01$ and $^{***}P<0.001$ vs the HK-2 group.

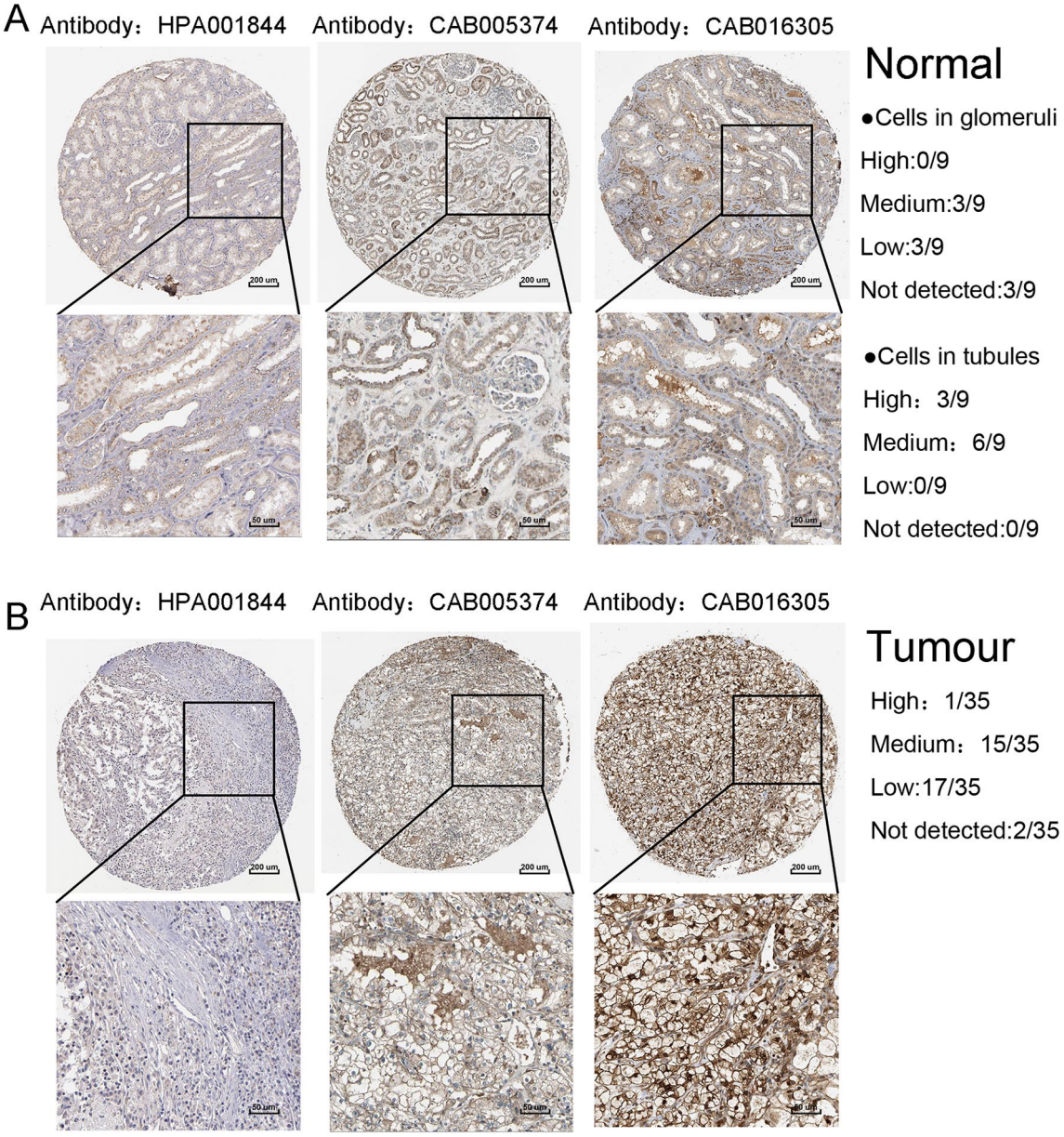

Fig. 3. Immunohistochemistry validation in ccRCC clinical specimens and para-carcinoma specimens. (**A**) Expression of SHC1 in para-carcinoma specimens of ccRCC patients. (**B**) Expression of SHC1 in ccRCC clinical tissues. Three antibodies (HPA001844, CAB005374, CAB016305) were applied. Scale bar = 200 μm.

Supplementary 5). The related functions of SHC1 were mainly B-cell receptor signaling pathway, phagocytosis recognition, immunoglobulin complex circulation, immunoglobulin receptor binding and collagen fibril organization (Fig. 5C). The associated pathways of SHC1 were chronic myeloid leukemia, ECM receptor interaction, NOD-like receptor signaling pathway, olfactory transduction and small cell lung cancer (Fig. 5D). It is noteworthy that ECM receptor interaction is a common pathway referring to both KEGG and GSEA analyses. We obtained the common pathway information related to SHC1 from the KEGG website (https://www.kegg.jp/) and labeled the genes associated with SHC1 in this pathway. The pathway diagram shows four genes (COL6A3, LAMC1, ITGB1 and ITGA5), all of which are positively correlated with SHC1. It is suggested that SHC1 could promote the activity of this signaling pathway.

Immune infiltration analysis

The present study focused on the relationship between SHC1 and tumor immune infiltration. Using the CIBERSORT method, 22 types of immune cells were explored, among which 9 kinds showed differences ($P < 0.05$, Fig. 6A). In addition, SHC1 was found to be correlated with 11 types of immune cells ($P < 0.05$, Fig. 6B), indicating that SHC1 may regulate various immune cells and affect the human immune response. Furthermore, ssGSEA was applied to study the association between SHC1 expression and the tumor immune microenvironment. The results revealed a significant increase in infiltration scores of 7 types of immune cells in the high SHC1 expression

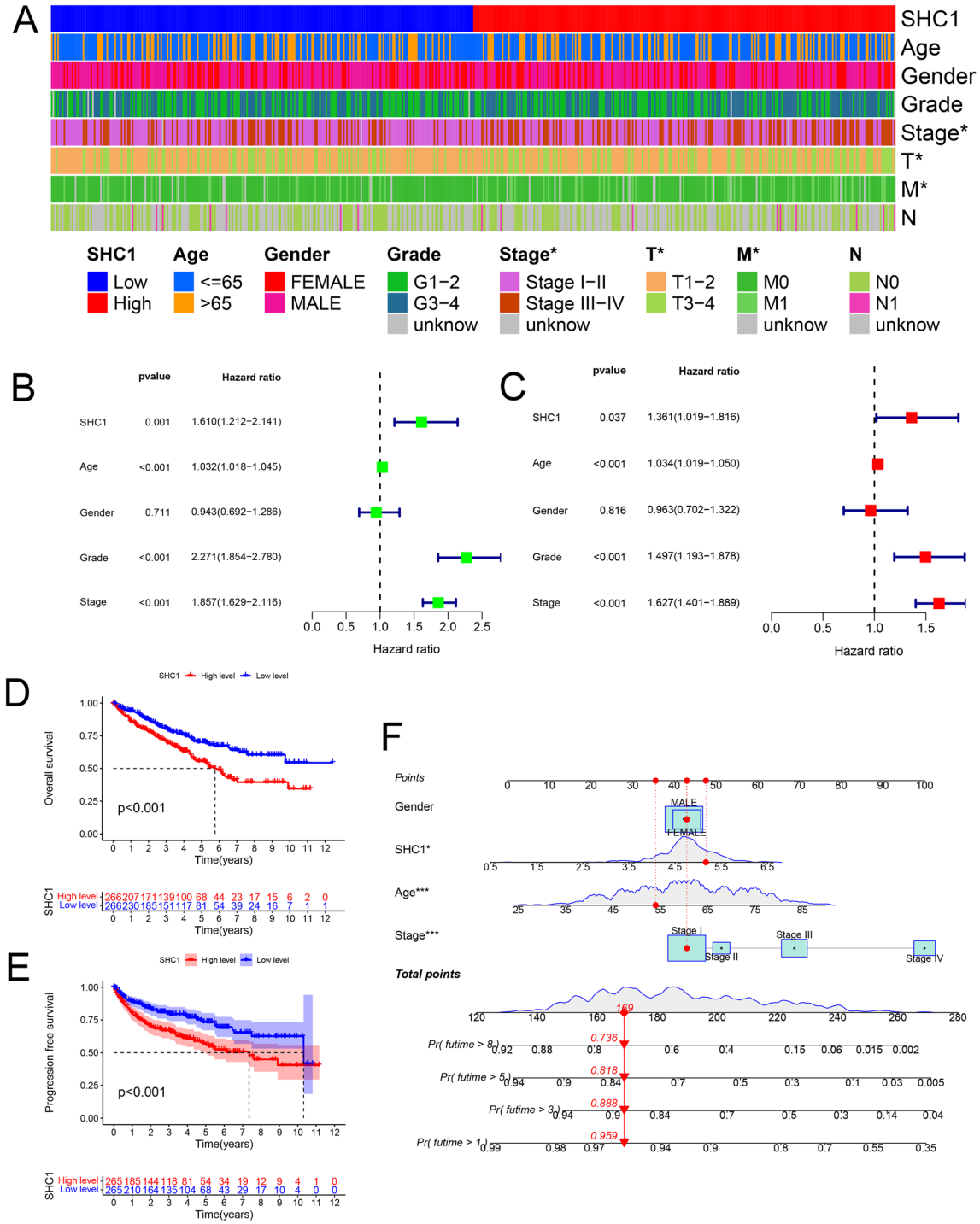

Fig. 4. Study on SHC1 expression and clinical correlation. (**A**) Differences in age, gender, grade, T Stage, N stage and M stage in high and low SHC1 expression. (**B**) Univariate analysis of the relationship between SHC1 expression and traditional clinical factors. (**C**) Multivariate analysis of the relationship between SHC1 expression and traditional clinical factors. (**D**) Kaplan–Meier survival curves of OS in different patient groups based on SHC1 expression. (**E**) Kaplan–Meier survival curves of PFS in different patient groups based on SHC1 expression. (**F**) A nomogram predicting 1 -, 3 -, 5- and 8-year OS based on ccRCC cohort from the TCGA database.

group ($P < 0.05$, Fig. 6C). Meanwhile, analysis of immune-related pathways demonstrated a significant elevation in scores of 7 immune pathways in the group with high expression of SHC1 ($P < 0.05$, Fig. 6D). All of these findings suggested a close relationship between the expression of SHC1 and immune infiltration.

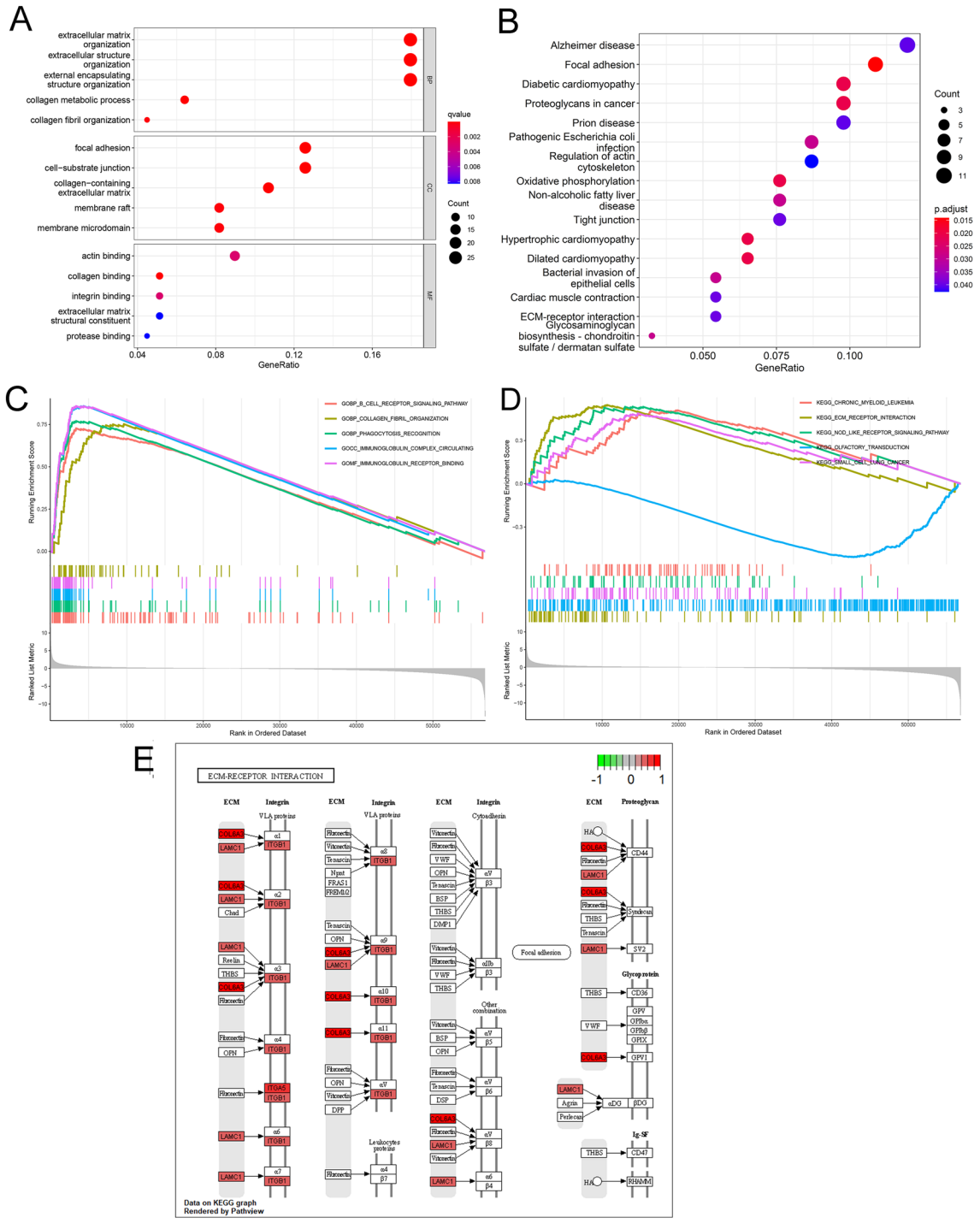

Fig. 5. Analysis of functions and pathways in ccRCC based on SHC1 expression. (**A**) GO enrichment analysis. The size of the circle represents the number of related genes (the larger the size is, the more related genes are discovered), and the color represents the P value (the redder, the smaller). (**B**) KEGG enrichment analysis. The size of the circle represents the number of related genes, and the color represents P value. (**C**) GSEA analysis showing functions in high- and low-expression of SHC1. (**D**) GSEA analysis showing pathways in high- and low-expression of SHC1. (**E**) The 'ECM-receptor interaction' pathway matched from the KEGG pathway database. In which the SHC1 related gene was stained. Positive correlation is red and negative correlation is green. The depth of the color represents the magnitude of the correlation.

Immune assessment and sensitivity to immunotherapy

Immune checkpoint is a reliable way to assess the patient's response to immunotherapy. We assessed differences

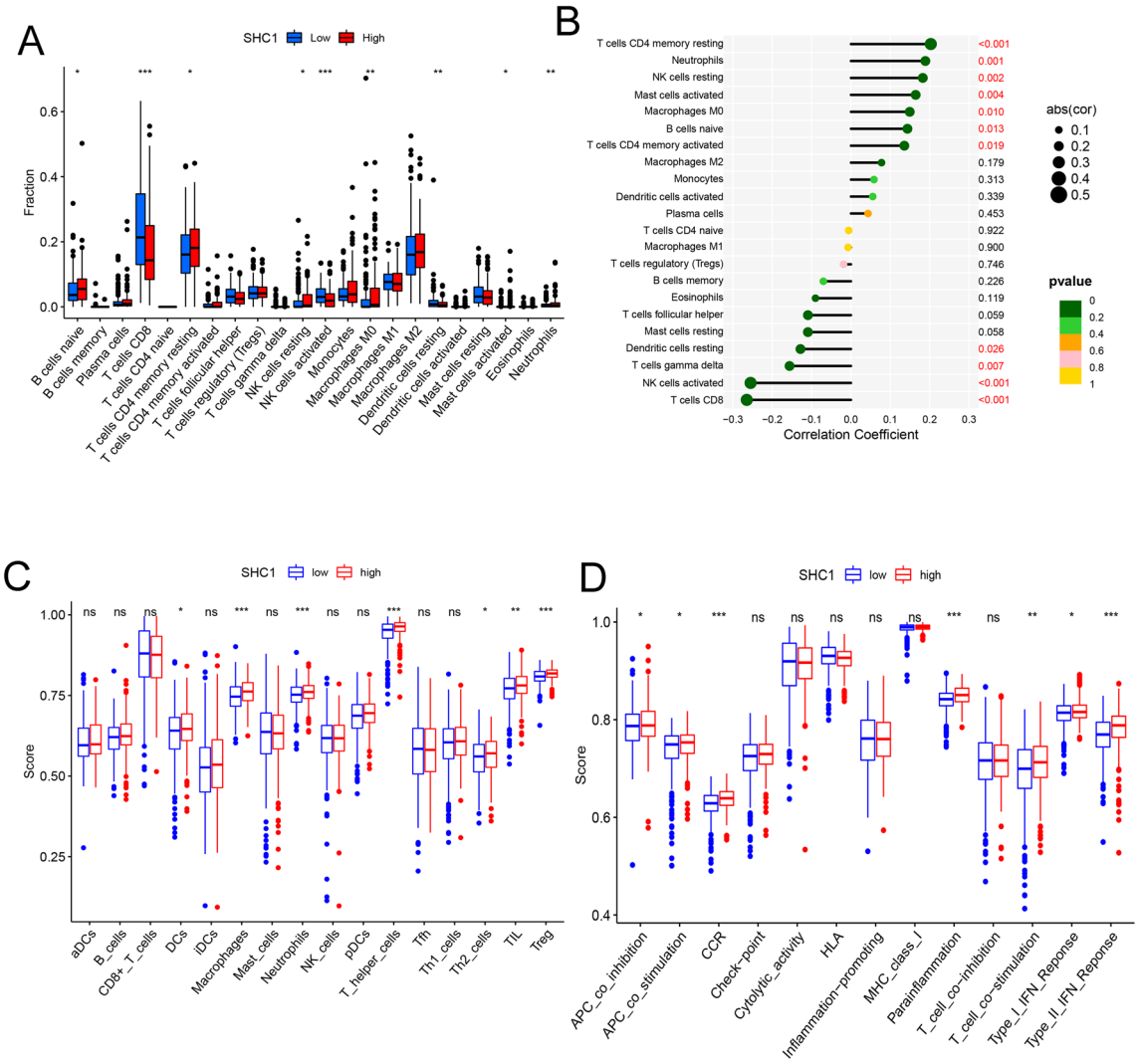

Fig. 6. Immune infiltration analysis of SHC1 in ccRCC. (**A**) Comparison of 22 types of immune cells in high- and low-expression of SHC1. (**B**) Correlation between SHC1 expression and 22 types of immune cells. (**C**) Comparison of ssGSEA scores of immune cells in high- and low-expression of SHC1. (**D**) Comparison of ssGSEA scores of immune-related pathways in high- and low-expression of SHC1.

in the expression of SHC1 referring to currently common immune checkpoints. The results indicate that in the group with high SHC1 expression, the expressions of CD80, CTLA4, PDCD1LG2 and VEGFA were up-regulated, while ERBB2 was down-regulated (see Fig. 7A)). With the assistance of TIDE database, we found that high expression of SHC1 is associated with higher TIDE, Excusion and Dysfunction scores, as well as lower MSI scores (Fig. 7B–E). This suggested that these patients with high-expressed SCH1 may not benefit as much from immunotherapy. In addition, we obtained immunophenoscores (IPS) from the TCGA-KIRC cohort from the TCIA database, which can predict the response to immunotherapy. According to the status of CTLA4 and PD1, all four subgroups with low expression of SHC1 exhibited significantly higher IPS scores (Fig. 7F–I), implying a potentially active response to immunotherapy. The low expression of SHC1 group was more sensitive to ICB treatment than the high expression group.

Discussion

It is widely accepted that ccRCC is one of the most common malignant tumors that threatens public health[16,17]. Traditional treatments (such as radical nephrectomy, partial nephrectomy and ablation) and some novel immunotherapies (such as ICIs and cytokines) have already been used in patients with ccRCC[18]. Surgical treatment is valuable to patients at early stage of ccRCC[19]. However, the effects of surgery are not satisfactory for patients who have progressed to advanced stages. Although molecular targeted drugs and immunotherapies have led to promising survival times and improved the quality of life in patients with advanced ccRCC[20], it remains obscure which group of patients would respond to the therapy better.

Previous studies have shown that immune genes are potential biomarkers and effective therapeutic targets for ccRCC immunotherapy[21]. Researchers have found that the immune gene SHC1 is strongly associated with the progression of lung, breast, pancreatic, and bladder cancers[22–24]. Furthermore, the expression level of SHC1

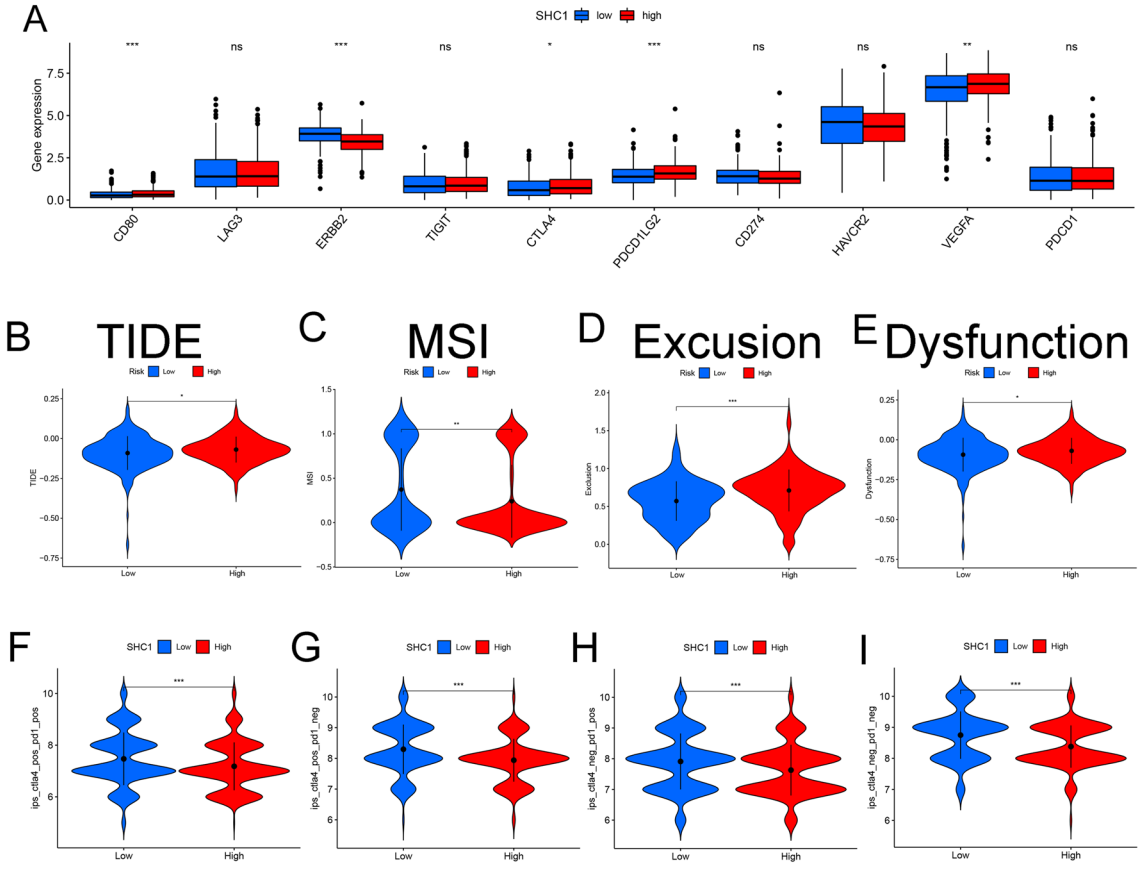

Fig. 7. Immune assessment and sensitivity to immunotherapy of SHC1. (**A**) Expression of common immune checkpoints in high- and low- expression of SHC1. (**B**) Distribution of SHC1 expression in TIDE scores. (**C**) Distribution of SHC1 expression in MSI scores. (**D**) Distribution of SHC1 expression in T-cell exclusion scores. (**E**) Distribution of SHC1 expression in T-cell dysfunction scores. (**F**) Distribution of SHC1 expression in CTLA4-positive and PD1-positive scores. (**G**) Distribution of SHC1 expression in CTLA4-positive and PD1-negative scores. (**H**) Distribution of SHC1 expression in CTLA4-negative and PD1-positive scores. (**I**) Distribution of SHC1 expression in CTLA4-negative and PD1-negative scores.

was seen to be elevated in ccRCC[15,25]. Nevertheless, the association between SHC1 and the prognosis of patients with ccRCC remains unclear, and whether SHC1 could provide immunotherapeutic value or not are still vague. In this study, we used bioinformatics analysis as well as experiments to explore the merits of SHC1 in ccRCC.

The level of SHC1 expression is increased in most cancer types. For example, Yang et al.[22] reported that SHC1 was highly-expressed in lung cancer. Wright et al.[23] displayed that increased SHC1 expression levels in breast cancer. Lai et al.[10] also showed an increased expression level of SHC1 in bladder cancer. These studies suggest that SHC1 may have a potential role in tumorigenesis. However, the mechanism of SHC1 in ccRCC has not yet been studied. In the present study, we aimed to reveal the expression and clinical relevance of SHC1 in the TCGA-KIRC cohort. The TCGA results indicate that the mRNA expression level of SHC1 was increased in ccRCC compared to normal tissues. Besides, multiple public databases validated our findings consistently. In addition, the results were validated against the patients with poor survival outcomes who had higher SHC1 expression. Hence it is speculated that SHC1 might function as a prognostic marker and a target for immunotherapy in ccRCC patients.

To strengthen our results discovered from bioinformatics, we collected samples from ccRCC patients and cell lines for confirmation. It is inspiring that SHC1 was proven to be upregulated in ccRCC patients and renal cancer cell lines (cell lines: 786-O, ACHN, and OS-RC-2) compared with adjacent tumor samples and normal kidney cells (HK-2). These results from in vitro experiments are consistent with previous results from bioinformatics analyses.

Kaplan–Meier analysis was performed on clinical information and sequencing data from public databases, aiming to explore the prognostic potential of SHC1 in KIRC. The results suggest that high levels of SHC1 predict poor survival outcomes in patients with ccRCC. Univariate and multivariate Cox regression analyses further validated these results, suggesting that SHC1 could be an independent predictor of survival in patients with ccRCC. Moreover, a nomogram combining SHC1 and other clinical factors was established to judge the OS of every patient precisely. Step by step, we tried to uncover the possible mechanism of SHC1 influencing survival outcome by GSEA enrichment analysis. We note that SHC1 may play an important role in ccRCC through the following signaling pathways: the B cell receptor signaling pathway, phagocytosis recognition, immunoglobulin

complex circulation, immunoglobulin receptor binding and collagen fibril organization, etc. These discoveries point out that SHC1 could affect the prognosis of ccRCC by modulating the level of immune cell response and immune infiltration. Therefore, we speculate that tumor development may be related to immune invasion induced by up-regulation of SHC1. More studies are needed to verify the mechanism of SHC1 in ccRCC.

The immune microenvironment plays an important role in the progression of ccRCC. It has been reported that the infiltration level of immune cells such as macrophages, T cells, and T follicular helper (Tfh) cells was associated with the prognosis of ccRCC[26–28]. GSEA shows that the function of SHC1 is related to various kinds of immune processes. We conducted analyses applying CIBERSORT and ssGSEA to further confirm the potential role of SHC1 in tumor immune microenvironment. The results show that the expression level of SHC1 is correlated with the infiltration levels of resting memory CD4 T^+ cells, neutrophils, resting NK cells, activated mast cells, M0 macrophages, naive B cells, activated memory CD4 T cells, resting dendritic cells, gamma delta T cells, activated NK cells, and CD8 T cells. The results via two different algorithms (CIBERSORT and ssGSEA) both showed that different levels of immune cell infiltration were exhibited in different expression levels of SHC1, suggesting that SHC1 might play vital roles in the tumor immune microenvironment.

It is a revolution when immune checkpoint inhibitors (ICIs) were applied in clinical treatment of multiple tumors[29,30]. Anti-programmed death receptor 1 (PD-1) therapy has been proven to improve the prognosis in ccRCC, especially those at an advanced or metastatic stage[31–33]. We also found that the expression of many ICI genes was related to SHC1 expression. Therefore, we consider that differential expression of SHC1 may contribute to tumor immunotherapy. Afterwards, we analyzed the value of SHC1 for immunotherapy in ccRCC using two approaches. TIDE algorithm can predict immune checkpoints blocking ICB treatment response[34]. Our results showed that patients with high expression of SHC1 had higher TIDE scores. Therefore, the phenomenon of a the lower ICB response in this group may be due to their T-cell dysfunction. TCIA analysis indicated that the group with low expression of SHC1 had a stronger immunotherapy response. This suggests that patients with low expression of SHC1 may benefit more from ICIs therapy than those with high expression levels. Regardless, we have to admit that our study lacks of clinical ccRCC immunotherapy cohort validation. Certainly, we are looking forward to multi-center clinical recruitment in the future.

Conclusions

In this study, bioinformatics analysis and experiments indicated that SHC1 could serve as a novel prognostic indicator in ccRCC. Besides, it also revealed the immune infiltration and immunotherapy value of SHC1 in ccRCC. We believe our study can provide new insights into the therapy of ccRCC. Of course, more evidence and further experiments are needed to confirm our findings.

Data availability

The datasets generated and analyzed during the current study are available from TCGA at https://portal.gdc.cancer.gov/, ICGC at http://dcc.icgc.org, GEO at https://www.ncbi.nlm.nih.gov/geo/, GTEx at https://gtexportal.org/home/ and CCLE at https://sites.broadinstitute.org/ccle. The authors confirm that the data supporting the findings of this study are available in the article and supplementary material.

Received: 8 February 2024; Accepted: 22 August 2024
Published online: 30 August 2024

References

1. Sung, H. *et al.* Global Cancer Statistics 2020: Globocan estimates of incidence and mortality worldwide for 36 cancers in 185 countries. *CA Cancer J. Clin.* **71**, 209–249 (2021).
2. Wolf, M. M., Kimryn, R. W. & Beckermann, K. E. Modeling clear cell renal cell carcinoma and therapeutic implications. *Oncogene* **39**, 3413–3426 (2020).
3. Ljungberg, B. *et al.* European Association of Urology guidelines on renal cell carcinoma: The 2019 update. *Eur. Urol.* **75**, 799–810 (2019).
4. Hegde, P. S. & Chen, D. S. Top 10 challenges in cancer immunotherapy. *Immunity* **52**, 17–35 (2020).
5. Senbabaoglu, Y. *et al.* Tumor immune microenvironment characterization in clear cell renal cell carcinoma identifies prognostic and immunotherapeutically relevant messenger Rna signatures. *Genome Biol.* **17**, 231 (2016).
6. Motzer, R. J. *et al.* Avelumab plus axitinib versus sunitinib for advanced renal-cell carcinoma. *N. Engl. J. Med.* **380**, 1103–1115 (2019).
7. Liu, C., Xiong, W., Song, J., Ouyang, X. & Fu, Y. Identification of immune-related seven-long non-coding RNA signature for overall survival and validation of the effect of Linc01270 in malignant phenotypes of clear cell renal carcinoma. *Cancer Manag. Res.* **15**, 131–145 (2023).
8. Pan, Z. *et al.* Bioinformatics analysis of immune-related prognostic genes and immunotherapy in renal clear cell carcinoma. *PLoS ONE* **17**, e272542 (2022).
9. Pelicci, G. *et al.* A novel transforming protein (Shc) with an Sh2 domain is implicated in mitogenic signal transduction. *Cell* **70**, 93–104 (1992).
10. Lai, C. H. *et al.* Depdc1B is a tumor promotor in development of bladder cancer through targeting Shc1. *Cell Death Dis.* **11**, 986 (2020).
11. Campbell, K. S. *et al.* Polyoma middle tumor antigen interacts with shc protein via the Npty (Asn-Pro-Thr-Tyr) motif in middle tumor antigen. *Proc. Natl. Acad. Sci. U. S. A.* **91**, 6344–6348 (1994).
12. Liang, Y. *et al.* The increased expression and aberrant methylation of shc1 in non-small cell lung cancer: Integrative analysis of clinical and bioinformatics databases. *J. Cell. Mol. Med.* **25**, 7039–7051 (2021).
13. Yang, Y. *et al.* Angiogenesis-related immune signatures correlate with prognosis, tumor microenvironment, and therapeutic sensitivity in hepatocellular carcinoma. *Front. Mol. Biosci.* **8**, 690206 (2021).
14. Hu, B., Yang, X. B. & Sang, X. T. Development of an immune-related prognostic index associated with hepatocellular carcinoma. *Aging (Albany NY).* **12**, 5010–5030 (2020).
15. Zhao, Y. *et al.* Ptrf/Cavin1, regulated by Shc1 through the egfr pathway, is found in urine exosomes as a potential biomarker of Ccrcc. *Carcinogenesis* **41**, 274–283 (2020).

16. Choueiri, T. K. *et al.* Inhibition of Hypoxia-inducible factor-2alpha in renal cell carcinoma with belzutifan: A phase 1 trial and biomarker analysis. *Nat. Med.* **27**, 802–805 (2021).
17. Znaor, A., Lortet-Tieulent, J., Laversanne, M., Jemal, A. & Bray, F. International variations and trends in renal cell carcinoma incidence and mortality. *Eur. Urol.* **67**, 519–530 (2015).
18. Motzer, R. J. *et al.* Kidney cancer, Version 3.2022, Nccn clinical practice guidelines in oncology. *J. Natl. Compr. Cancer Netw.* **20**, 71–90 (2022).
19. Ljungberg, B. *et al.* European Association of Urology guidelines on renal cell carcinoma: The 2022 update. *Eur. Urol.* **82**, 399–410 (2022).
20. Srivastava, A., Doppalapudi, S. K., Patel, H. V., Srinivasan, R. & Singer, E. A. The roaring 2020S: A new decade of systemic therapy for renal cell carcinoma. *Curr. Opin. Oncol.* **34**, 234–242 (2022).
21. Wang, Q. *et al.* Immune-associated gene signatures serve as a promising biomarker of immunotherapeutic prognosis for renal clear cell carcinoma. *Front. Immunol.* **13**, 890150 (2022).
22. Yang, P., Li, W. & Li, X. Shc1 Promotes lung cancer metastasis by interacting with Egfr. *J. Oncol.* **2022**, 3599832 (2022).
23. Wright, K. D. *et al.* The P52 isoform of Shc1 is a key driver of breast cancer initiation. *Breast Cancer Res.* **21**, 74 (2019).
24. Hamada, S., Masamune, A., Miura, S., Satoh, K. & Shimosegawa, T. Mir-365 induces gemcitabine resistance in pancreatic cancer cells by targeting the adaptor protein Shc1 and Pro-apoptotic regulator bax. *Cell. Signal.* **26**, 179–185 (2014).
25. Hua, X., Chen, J., Su, Y. & Liang, C. Identification of an immune-related risk signature for predicting prognosis in clear cell renal cell carcinoma. *Aging (Albany NY).* **12**, 2302–2332 (2020).
26. Su, S., Akbarinejad, S. & Shahriyari, L. Immune Classification of Clear Cell Renal Cell Carcinoma. *Sci Rep.* **11**, 4338 (2021).
27. Wang, Y., Yin, C., Geng, L. & Cai, W. Immune infiltration landscape in clear cell renal cell carcinoma implications. *Front. Oncol.* **10**, 491621 (2020).
28. Chevrier, S. *et al.* An immune atlas of clear cell renal cell carcinoma. *Cell* **169**, 736–749 (2017).
29. Joshi, S. S. & Badgwell, B. D. Current treatment and recent progress in gastric cancer. *CA-Cancer J. Clin.* **71**, 264–279 (2021).
30. Pardoll, D. M. The blockade of immune checkpoints in cancer immunotherapy. *Nat. Rev. Cancer.* **12**, 252–264 (2012).
31. Rathmell, W. K. *et al.* Management of metastatic clear cell renal cell carcinoma: Asco guideline. *J. Clin. Oncol.* **40**, 2957–2995 (2022).
32. Braun, D. A. *et al.* Interplay of somatic alterations and immune infiltration modulates response to Pd-1 blockade in advanced clear cell renal cell carcinoma. *Nat. Med.* **26**, 909–918 (2020).
33. Miao, D. *et al.* Genomic correlates of response to immune checkpoint therapies in clear cell renal cell carcinoma. *Science* **359**, 801–806 (2018).
34. Jiang, P. *et al.* Signatures of T cell dysfunction and exclusion predict cancer immunotherapy response. *Nat. Med.* **24**, 1550–1558 (2018).

Author contributions

Z.G: Conceptualization, Methodology, Visualization, Writing—original draft. C.C: Conceptualization, Data curation, Funding acquisition, Methodology, Software, Validation, Writing—original draft. K.Z: Formal Analysis, Writing—original draft. L.S: Investigation, Writing—review & editing. XW: Investigation, Writing—review & editing. D.C: Data curation, Resources, Visualization, Writing—review & editing. G.W: Conceptualization, Funding acquisition, Project administration, Resources, Supervision, Validation, Writing—review & editing. S.H: Data curation, Funding acquisition, Methodology, Project administration, Validation, Writing—original draft, Writing—review & editing.

Funding

This work was supported by grants from the Zhejiang Province Medical and Health Science and Technology Plan Project (No. 2024KY1065), Zhejiang Province Traditional Chinese Medicine Science and Technology Plan Project (No. 2023ZL669) and Yinzhou District Health Science and Technology Plan Project (No.202045, No.2023Y08 and No.2023AS062).

Competing interests

The authors declare no competing interests.

Additional information

Supplementary Information The online version contains supplementary material available at https://doi.org/10.1038/s41598-024-70897-3.

Correspondence and requests for materials should be addressed to G.W. or S.H.